Involvement of structurally distinct cupuassu chitinases and osmotin in plant resistance to the fungus Moniliophthora perniciosa

Raner José Santana Silva, Rafael Moyses Alves, Karina Peres Gramacho, Lucilia Helena Marcellino, Fabienne Micheli

Involvement of structurally distinct cupuassu chitinases and osmotin in plant resistance to the fungus *Moniliophthora perniciosa*

Raner José Santana Silva[1], Rafael Moyses Alves[2], Karina Peres Gramacho[3], Lucilia Helena Marcellino[4], Fabienne Micheli[1,5,*]

[1]Universidade Estadual de Santa Cruz (UESC), Departamento de Ciências Biológicas (DCB), Centro de Biotecnologia e Genética (CBG), Rodovia Ilhéus-Itabuna, km 16, 45662-900 Ilhéus-BA, Brazil.

[2]Empresa Brasileira de Pesquisa Agropecuária, Embrapa Amazônia Oriental, 66095-903 Belém-PA, Brazil.

[3]Cocoa Research Center, CEPLAC/CEPEC, 45600-970 Itabuna-BA, Brazil.

[4]Empresa Brasileira de Pesquisa Agropecuária, Embrapa Recursos Genéticos e Biotecnologia, Brasília-DF, 70770-917, Brazil.

[5]CIRAD, UMR AGAP, F-34398 Montpellier, France.

***Corresponding author:** Dr Fabienne Micheli, UESC, DCB, Rodovia Ilhéus-Itabuna km16, 45662-900, Ilhéus-BA, Brazil. Phone: +55 73 3680 5196. Fax: +55 73 3680 5226. E-mail: fabienne.micheli@cirad.fr

Abstract:

The cupuassu tree (*Theobroma grandiflorum*) is a crop of great economic importance to Brazil, mainly for its pulp and seeds, which are used in food industry. However, cupuassu fruit production is threatened by witches' broom disease caused by the fungus *Moniliophthora perniciosa*. As elements of its defense mechanisms, the plant can produce and accumulate

pathogenesis-related (PR) proteins such as chitinases and osmotins. Here, we identified three PR proteins from cupuassu (TgPR3, TgPR5 and TgPR8) from cupuassu-*M. perniciosa* RNA-seq data. TgPR3 and TgPR8 corresponded to chitinases, and TgPR5 to osmotin; they are phylogenetically related to cacao and to Arabidopsis PR sequences involved in biotic and abiotic stress. The TgPR proteins' tridimensional structure was obtained through homology modeling, and molecular docking with chitin and chitosan showed that the TgPR proteins can interact with both cell wall molecules and presented a higher affinity for chitosan. TgPR gene expression was analyzed by RT-qPCR on resistant and susceptible cupuassu genotypes infected by *M. perniciosa* at 8, 24, 48 and 72 hours after infection (hai). The TgPR genes showed higher expression in resistant plants compared to the susceptible ones, mainly for TgPR5 at 8 and 24 hai, while the expression was lower in the susceptible cupuassu plants. To our knowledge, this is the first *in silico* and *in vitro* reports of cupuassu PR protein. The data suggested that TgPRs could be involved in recognizing mechanisms of the plant's innate immune system through chitin receptors. Our results also suggest a putative role of chitinase/chitosanase for the TgPR5/osmotin.

Keywords: Pathogenesis-related proteins, molecular docking, witches' broom disease, gene expression, chitin, chitosan

1. Introduction

The cupuassu (*Theobroma grandiflorum* [Willd. Ex Spreng.] Schum.) belongs to the Malvaceae family; it is native to the Amazon region and is economically important to Brazil, where it is cultivated [1, 2]. Cupuassu pulp and seeds are used in the cosmetics and food industries, mainly for candy, ice cream, beverage and *cupulate* (a product similar to chocolate) production [3]. *Cupulate* is an interesting alternative to chocolate production for an

actual worldwide economic situation in which the production of cocoa (*Theobroma cacao*, Malvaceae family) beans cannot supply the increased worldwide demand for chocolate [4, 5]. However, both cocoa and cupuassu cultures are affected by pests and pathogens that cause damage, loss of production and even plant death. Among them, witches' broom disease, caused by the fungus *Moniliophthora perniciosa*, is the main phytopathological problem for cupuassu cultures [6].

Because they are attacked by a wide variety of pathogens, plants have developed pattern-recognition receptors to recognize molecular patterns associated with pathogens (PAMPs), which lead, among other outcome, to the production and accumulation of pathogenesis-related proteins (PR proteins), which are considered crucial to plant defense mechanisms [7-9]. The current classification divides PR proteins into 17 classes (PR1–PR17) depending on their biological activity, physicochemical properties and/or sequence homology [10, 11]. The PR-3, PR-4, PR-8 and PR-11 families correspond to different types of chitinases (EC 3.2.1.14). Among them, the PR-3 proteins include glycoside hydrolase 19 (GH19) chitinases, and the PR-8 family corresponds to glycoside hydrolase 18 (GH18) chitinases. The PR-5 family classification corresponds to thaumatin-like protein (TLPs), whose biological function in plants has yet to be established [12]. Among TLPs, the osmotins are multifunctional proteins that may participate alongside chitinases in protein complexes involved in plant defense against pathogens [8, 13]. GH18, GH19 and osmotin show antifungal activity through cell wall hydrolysis or plasma membrane permeabilization [12, 14]; in the case of PR-5, it has been proposed that the existence of specific target receptors on the membrane leads to fungus sensitivity or resistance [15]. The GH18 chitinases show a characteristic barrel structure [16], while GH19 chitinases are composed of a high concentration of α-helices and loops [14]. The TLP proteins have three well-characterized domains: domain I is composed of β sheets and loops called a β-sandwich, domain II is

composed of α-helices and domain III is composed of two β-sheets [17]. Because chitin is present in the fungus cell wall and not in plant cells, it is considered an ideal PAMP and as one of the first barriers in the plant-pathogen battlefield [18, 19]. Chitin and chitosan, its deacetylated derivative, have been heavily studied, and their role in plant–pathogen interaction has received considerable attention, mainly because they are considered useful for biotechnological applications aimed at reducing fungus activity and/or development [19-21]. *Moniliophthora perniciosa*'s chitin metabolism, including associated enzymes such as chitin synthases and chitinases, has previously been studied [22-25].

Molecular studies of cupuassu related to plant–pathogen interaction are still poorly developed, and few works are related to resistance to witches' broom disease [26-28]. Moreover, unlike cocoa, the cupuassu genome has not been sequenced yet, and molecular analyses focused on genetics and genomics of resistance are only based on recent transcriptomic data [26, 28]. Here, we selected and analyzed three PR genes from cupuassu (TgPR3, TgPR5 and TgPR8) with putative chitinase or chitinase-associated functions as well as anti-fungal activity. We showed, *in silico*, the TgPR proteins' structural aspects and potential activity in relation to chitin and chitosan ligands, and, *in vitro*, the contrasting expression levels of the *TgPR* genes in resistant and susceptible cupuassu plants inoculated with *M. perniciosa*. Their expression profiles could be related to phylogenetic analysis using homologous PR sequences from *T. cacao* and *A. thaliana*, which are involved in response to biotic and abiotic stress. To our knowledge, this is the first PR protein report on cupuassu–*M. perniciosa* interaction. The overall data data suggest that TgPRs could be involved in recognizing mechanisms of the plant's innate immune system through chitin receptors. Our results also suggest a putative role of chitinase/chitosanase for the TgPR5/osmotin.

2. Methods

2.1 Identification and characterization of *TgPR* sequences

The PR sequences were selected from a previously obtained RNA-Seq database of cupuassu [28]. Open reading frame (ORF) detection was performed using the ORFinder software (http://www.ncbi.nlm.nih.gov/gorf/gorf.html). The proteins were analyzed with BLASTp against the Conserved Domain Database (CDD; https://www.ncbi.nlm.nih.gov/Structure/cdd/wrpsb.cgi) for conserved domain identification, protein sequence length checking and TgPR protein classification. Signal peptide was identified using the SignalP 4.1 software [29], while the molecular weight and isoelectric point were obtained using the Compute pI/Mw program [30]. The subcellular locations were predicted using the YLoc-HighRes Plants tool [31].

2.2 Phylogeny

Cacao and Arabidopsis nucleotide sequences that are homologous to TgPRs were obtained using local alignment (BLAST) from CocoaGenDB [32] and TAIR (https://www.arabidopsis.org), respectively. The global multiple alignment of all sequences was made using ClustalW available with MEGAX software [33]. The MEGAX software was used to construct a rooted phylogenetic tree using the maximum likelihood method with 1,000 bootstrap sampling steps, the Tamura-Nei model and the G+I substitution method. Phylogenetic trees were visualized and edited using the FigTree v1.4.4 tool (http://tree.bio.ed.ac.uk/software/figtree/).

2.3 Homology modeling of TgPRs and molecular docking with chitin and chitosan

The tri-dimensional (3D) structure of the TgPR proteins was obtained using the Swiss-Model server [34]. The crystal structures of homologous proteins available from the Protein Data Bank (PDB; https://www.rcsb.org/) were used as templates to build the structural models of

TgPR (Supplementary material 1). The stereochemical quality of the models was analyzed with ANOLEA [35] and Procheck [36]. Water molecules were removed from and polar hydrogens were added to the TgPR protein models, before calculation of their Gasteiger charges; the results were exported in PDBQT format. The active sites were identified based on TgPR protein alignment with PR proteins from other species (Supplementary materials 2 to 4), using the ClustalW tool [37]. The amino acid residues from the TgPR active sites of the proteins as well as the grid box defining the docking region were marked using AutoDock Tools v1.5.6 [38]. For docking, chitin (CID: 444514) and chitosan (CID: 71853) were used as ligands; their structures were downloaded in SMILES format. Using the MarvinSketch 15.7.13.0 tool, the ligands were converted into 3D structures, checked for conformation and saved in mol2 format. The Kollman charges were calculated using AutoDockTools v1.5.6, and the results were exported in PDBQT format. The docking was done using the AutoDock Vina software [39] with default parameters. The results were visualized in PyMOL v1.7.4 [40] and Discovery Studio 4.5.

2.4 Plant material

TgPR gene expression was analyzed in adult plants obtained from clonal cuttings of cupuassu genotypes C174 (resistant to witches' broom disease) and C1074 (susceptible to witches' broom disease), grown in the experimental station of CEPLAC (Belém, Pará, Brazil) [41]. Cupuassu apical meristems were inoculated with *M. perniciosa* using the droplet method (30 µL of suspension containing $1x10^5$ ml^{-1} basidiospores) [42]. After inoculation, the stem apex region was wrapped in a plastic bag (a water-saturated environment) to improve basidiospore germination and plant infection by the fungus [43]. The control plants were submitted to the same procedure, but the basidiospore suspension was replaced by distilled water. The apical meristems of the inoculated C174 and C1074 genotypes were harvested 8, 24, 48 and 72

hours after inoculation (hai), while non-inoculated ones (control) were harvested at 8 hai Three plants (biological replicates) were used for each genotype at each harvesting time. The harvested samples were immediately frozen in liquid nitrogen and stored at −80 °C until use.

2.5 Reverse transcription quantitative PCR (qPCR) analysis

Each biological replicate (individual plant) was macerated in liquid nitrogen, and 3 mg of the macerate was used to extract its total RNA using the RNAqueous® kit according to the manufacturer's recommendations (Ambion). Total RNA (15 µl) was treated with the DNase I kit according to the manufacturer's recommendations (Invitrogen). The cDNA was synthesized using the RevertAid First Strand cDNA Synthesis Kit, a cDNA synthesis kit, according to the manufacturer's recommendations (ThermoScientific). The cDNA was quantified on a GeneQuant Pro Spectrophotometer UV/Vis Reader (Amersham). For qPCR, the *TgPR* primers were designed with the Primer 3 plus tool [44] using previously described parameters [45], and checked for dimer and hairpin formation using the Oligoanalyzer (https://www.idtdna.com/calc/analyzer) (Supplementary material 5). Three reference genes (acyl carrier protein/ACP, malate dehydrogenase/MDH and tubulin/TUB; Supplementary material 5) previously identified in cupuassu [27] were analyzed for stability in three pooled samples of each cupuassu genotype: i) a non-inoculated pool sample (3 plants); ii) a pool of 8 and 24 hai samples (6 plants); and iii) a pool of 48 and 72 hai samples (6 plants). Quantitative PCR was performed in an Eppendorf thermocycler Realplex4. The reaction was made in a final volume of 10 µl containing 5 µl of Taq READYMIX SYBR Green, 0.1 µl of ROX (fluorescence signal normalizer), 0.5 µl of primers (forward and reverse, at a concentration of 10 mM each) and 4.4 µl of cDNA 1/20 (230 ng). The cycling conditions were 95°C for 2 min followed by 45 cycles of 95°C for 15 s, 55°C for 15 s and 60°C for 45 s, followed by a dissociation curve step. The fluorescence data and primer efficiency were analyzed using

MINER 4.0 [46]. The gene-expression stability was calculated using NormFinder [47], which determined the best combination of the reference genes ACP and MDH for relative expression calculation (Supplementary material 6). The gene expression was analyzed in each biological replicate (1 biological replicate = 1 plant) for each genotype (inoculated vs. non-inoculated) at each harvesting time, using the qPCR cycling conditions described above and three technical replicates. The relative expression was obtained using the REST-2009 software [48], which considers the primer efficiency as well as the average ACP and MDH values for calculation.

3. Results

3.1 Identification and characterization of *TgPR* sequences

Analysis of the cupuassu RNA-seq allowed the selection of three sequences – codified as C106, C68 and C356 – and showed homology with chitinases [28]. Sequence C106 showed homology with chitinases from the GH19 family, which are involved in pathogenesis and are related to the PR3 class (Table 1). For this reason, sequence C106 was re-named as *T. grandiflorum* pathogenesis-related protein 3 (TgPR3). The *TgPR3* ORF was 966 bp in length and encoded for a 322 aa protein with a molecular weight and an isoelectric point of 35.5 kDa and 6.64, respectively (Table 1). TgPR3 contained a signal peptide (26 aa) responsible for extracellular addressing (86.48% of probability). The protein contained 17 and three predicted phosphorylation and glycosylation sites, respectively (Table 1). The C68 sequence showed homology with the thaumatin like protein (TLP-P) family, which belongs to the pathogenesis-related protein 5 (PR5) class and includes chitinases and osmotins. The C68 sequence was renamed *T. grandiflorum* pathogenesis-related protein 5 (TgPR5) (Table 1). The TgPR5's ORF was 672 bp in length, and it encoded a 224 aa protein with a molecular weight of 24.2 kDa and an isoelectric point of 6.68 (Table 1). The protein contained a 23 aa signal peptide responsible for extracellular addressing (99.7% probability). TgPR5 contains one predicted

glycosylation and eight predicted phosphorylation sites (Table 1). The protein encoded by the C356 sequence was classified as a chitinase from the GH18 family and as hevamine enzyme, which are chitinases belonging to the class of pathogenesis-related protein 8 (PR8). This sequence was renamed *T. grandiflorum* pathogenesis-related protein 8 (TgPR8). The TgPR8 ORF was 927 bp in length, and it encoded for a 309 aa protein with a molecular weight of 33.3 kDa and a pI of 4.27 (Table 1). TgPR8 contains a signal peptide (29 aa), which potentially addresses the protein to the extracellular (52.2% probability) or the vacuolar (34.5% probability) compartments. The TgPR8 protein showed one and 13 glycosylation and phosphorylation sites, respectively (Table 1).

3.2 Phylogeny

BLAST made from *TgPR* sequences allowed the identification of 11 and 14 homologous sequences of TgPR3, 30 and 28 of TgPR5 and 14 and one of TgPR8 in *T. cacao* and *A. thaliana*, respectively (Fig. 1). TgPR3 showed a high homology with *T. cacao* sequences Tc04_t029180 and Tc06_t000490 and with *A. thaliana* sequences AT3G16920.1 and AT1G05850.1 (Fig. 1A). TgPR5 was clustered with the sequences Tc00_t060970, Tc03_t026960, Tc03_t026980, Tc03_t026990, Tc03_t027000, Tc03_t027010 and Tc03_t027030 from *T. cacao* and with AT4G11650 (OSM34) from *A. thaliana* (Fig. 1B). TgPR8 was clustered with the sequences Tc01_t032120, Tc03_t017760, Tc03_t017780, Tc03_t017790, Tc10_t015260 and Tc10_t015330 from *T. cacao* as well as with AT5G24090 from *A. thaliana* (Fig. 1C).

3.3 Homology modeling and validation of TgPR's 3D structure

The TgPR3 protein's 3D structure (Fig. 2A) was obtained through homology modeling with the GH19 chitinase (PDB: 4TX7) from *Vigna ungiculata* (39% of identity and 91% of

226 coverage; Supplementary material 1). The TgPR3 protein 3D model showed that 87% of the
227 amino acid residues was in the most favored regions, 11.8% was in the additional allowed
228 regions, 0.6% was in the generously allowed regions and 0.6% was in the disallowed regions
229 (Supplementary material 7A). The TgPR3 model contained 12 helices, 26 β-turns, eight ɣ-
230 turns and three disulfide bonds (Fig. 2A, Supplementary material 8). The alignment of TgPR3
231 with other GH19 chitinases from other species (Supplementary material 2) allowed the
232 identification of TgPR3's catalytic site containing the amino acid residues Lys_{70}, Glu_{92} and
233 Tyr_{125} (Fig. 2A). The TgPR5 protein's 3D structure (Fig. 2B) was obtained by homology
234 modeling with an osmotin (PDB: 4L2J) from *Calotropis porcine* (75% of identity and 100%
235 of coverage; Supplementary material 1). The TgPR5 protein 3D model showed 88.5% of the
236 amino acid residues in the most favored regions, 11.1% in the generously allowed regions and
237 0.4% in the allowed regions, and it had no amino acid residues in disallowed regions
238 (Supplementary material 7B). The TgPR5 model contained 14 β-sheets, five helices, 25 β-
239 turns, two ɣ-turns, one bulge, five hairpins and seven disulfide bonds (Fig. 2B, Supplementary
240 material 8). The alignment of TgPR5 protein with thaumatine-like proteins from other species
241 (Supplementary material 3) allowed the identification of putative amino acid residues from
242 the active cleft: Arg_{43}, Glu_{83}, Asp_{96} and Asp_{101} (Fig. 2B). The TgPR8 protein's 3D structure
243 (Fig. 2C) was obtained by homology modeling with hevamine A (PDB: 1LLO) from *Hevea*
244 *brasiliensis* (64% of identity and 99% of coverage; Supplementary material 1). The TgPR8
245 protein's 3D structure showed 78.8% of the amino acid residues in the most favored regions,
246 18.9% in the additional allowed regions, 0.9% in the generously allowed regions and 1.4% in
247 disallowed regions (Supplementary material 7C). The TgPR8 model contained a barrel shape
248 with nine β-sheets, 15 helices, three disulfide bonds, 16 β-turns, one ɣ-turn, four bulges, one
249 hairpin, six α-β units and one PSI loop (Fig. 2C, Supplementary material 8). The alignment of
250 TgPR8 with GH18 chitinases from other species (Supplementary material 4) allowed the

identification of motifs and conserved domains, including the predicted active site containing the amino acid residues Tyr_{6}, Phe_{32}, Asp_{125}, Glu_{127}, Gln_{155}, Gln_{178}, Tyr_{180} and Trp_{253} (Fig. 2C).

3.4 Molecular docking between TgPRs and chitin or chitosan

The molecular docking of TgPR3 with chitin had an affinity energy of −6.4 kcal/mol (Supplementary material 9). It showed conventional hydrogen bond interactions with amino acid residues Ser_{92}, Gly_{94}, Glu_{112} and Tyr_{225}, and carbon hydrogen bonds with amino acid residues Lys_{90} and Pro_{217} (Fig. 3). The molecular docking of TgPR3 with chitosan had an affinity energy of −7.4 kcal/mol (Supplementary material 9). It showed conventional hydrogen bond interactions with amino acid residues Lys_{90}, Ser_{92}, Asp_{118}, Tyr_{119}, Tyr_{145}, Tyr_{148}, Arg_{182}, Leu_{224}, Tyr_{225} and Asp_{236}; carbon hydrogen bonds with amino acid residues Thr_{91}, Tyr_{109} and Arg_{111}; and alkyl interactions with the amino acid residue Pro_{143} (Fig. 3). The molecular docking of TgPR5 with chitin had an affinity energy of −6.5 kcal/mol (Supplementary material 9) and showed conventional hydrogen bonds with the amino acid residues Thr_{40}, Glu_{83}, Gln_{88}, Asp_{96} and Pro_{179}; one carbon hydrogen bond with the amino acid residue Asp_{182}; and one pi-sigma interaction with the amino acid residue Tyr_{176} (Fig. 3). The molecular docking of TgPR5 with chitosan had an affinity energy of −6.8 kcal/mol (Supplementary material 9) with conventional hydrogen bonds in the amino acid residues Thr_{40}, Ala_{42}, Tyr_{74}, Gly_{75}, Glu_{83}, Tyr_{84}, Asp_{96}, Asp_{101}, Tyr_{176} and Asp_{182} and one carbon hydrogen bond in the amino acid residue Cys_{154} (Fig. 3). The molecular docking of TgPR8 with chitin had an affinity energy of −7.0 kcal/mol (Supplementary material 9) and showed conventional hydrogen bonds with the amino acid residues Gln_{9}, Ala_{81}, Glu_{127}, Gln_{155}, Tyr_{180} and Tyr_{257} (Fig. 3). The docking of TgPR8 with chitosan had an affinity energy of −7.3 kcal/mol (Supplementary material 9) and showed conventional hydrogen bonds with the

amino acid residues Gln_9, Ser_{43}, Met_{44}, Asn_{45}, Leu_{46}, Gln_{155}, Asn_{181}, Asn_{182}, Ala_{221}, Trp_{253} and Tyr_{257}, and carbon hydrogen bonds with the amino acid residues Gln_{178} and Tyr_{180} (Fig. 3).

3.5 Analysis of *TgPR* gene expression

The primers PR3, PR5, PR8, ACP and MDH showed efficiency from 91% (MDH on the C1074 genotype) to 102% (P3 on both the C174 and C1074 genotypes; Supplementary material 10). For both genotypes and for all of the harvesting points, the PCR amplification occurred at the same and unique melting temperature for each gene and a unique band was visible on electrophoresis agarose gel, showing that only the corresponding gene was amplified (Supplementary material 11). The relative expression of the *TgPR* genes was lower in the susceptible genotype at all of the harvesting times, as compared to the resistant genotype (Figs. 4A and B). The *TgPR3* gene showed two to three times higher expression in the resistant genotype than in the susceptible one (Fig. 4B). Similarly, the *TgPR8* gene showed two to four times higher expression in the resistant plants compared to the susceptible ones (Fig. 4B). For both the *TgPR3* and *TgPR8* genes, the expression through the time course disease slightly increased from 8 to 72 hai in the resistant plants (Fig. 4B). The *TgPR5* gene showed a very high expression at 8 and 24 hai in the resistant genotype (about 25 of relative expression; Fig. 4A), which decreased at 48 and 72 hai (about 2 of relative expression; Fig. 4B). Except for *TgPR5* 8 hai, the relative expression of the *TgPR* genes in the susceptible genotype was almost constant (Fig. 4B).

4. Discussion

4.1 TgPRs are structurally distinct and show a high energy affinity for chitosan

The TgPR3 and TgPR5 proteins showed similar isoelectric points and share the same cellular addressing (extracellular; Table 1), whereas the TgPR8 protein shows a more acidic

isoelectric point. Although the predictions for TgPR8 suggested extracellular and vacuolar addressing (Table 1), type GH18 chitinases are found in the apoplast [49]. Although GH19 (PR-3) chitinases are composed of α-helices and loops, they are highly thermostable [50]. GH19 are divided into loopful and loopless classes, where loopful chitinases have loops at both ends of the substrate-binding site, while loopless chitinases have a non–end loop structure, which is commonly found in bacteria [51]. The TgPR3 protein showed homology with the loopful GH19 class because of the presence of the loops near the substrate-binding site (Fig. 2A). Most GH18 proteins (PR-8) correspond to chitinases, although some have been reported to have xylanase-inhibiting activity or to have lost their chitinase activity [16]. As chitinases, the GH18 proteins have the same activity as GH19 but are extremely distinct, both structurally and evolutionarily [52]. One pattern that defines the chitinase activity in GH18 is the presence of a DXDXE motif [53]; the TgPR8 showed the DFDIE motif at positions 123–127 of the sequence, corroborating its classification and potential chitinase activity (Supplementary material 8). Osmotin antifungal activity is associated with the presence of the acidic cleft region [15, 54], which in TgPR5 protein is composed of the residues Glu_{83}, Asp_{96} and Asp_{101} (Figure 1B). *In vitro* studies have shown that barley seeds' GH19 chitinase can efficiently catalyze tetrameric N-acetylglucosamine in dimers but that most GH19 chitinases prefer larger substrates [55]. These data corroborate our docking results, where the TgPR3 protein had an affinity of −6.4 kcal/mol with the chitin molecule (the smaller one) and −7.4 kcal/mol with the chitosan molecule (the larger one), showing that TgPR3 also has a higher affinity for larger substrates (Supplementary material 9, Fig. 3). TgPR8 protein has similar affinity energy for chitin and chitosan ligands (−7.0 kcal/mol and −7.3 kcal/mol, respectively; Supplementary material 9). The docking results reinforced the putative TgPR8 protein chitinase activity, with an interaction within the DFDIE motif, in which it is essential for the chitinase activity of this protein class [53]. Although structurally different and having

different catalytic mechanisms [52], the proteins TgPR3 and TgPR8 have a very close affinity energy for the chitosan molecule. This may be related to their activity type, as both are glycoside hydrolases [56]. The TgPR5 protein had an affinity energy of −6.5 kcal/mol with the chitin molecule and −6.8 kcal/mol with the chitosan molecule (Supplementary material 9; Fig. 3). These results show that TgPR5 can bind chitin molecules and may have potential chitinase and antifungal activity.

4.2 TgPRs are homologous to other plant PR proteins involved in biotic and abiotic stress

TgPR3 was clustered with Tc06_t000490 and Tc04_t029180 (Fig. 1), which showed a high constitutive expression across treatments, Tc06_t000490 being up-regulated during cacao-*Phytophthora palmivora* interaction [57]. The AT3G16920 from *A. thaliana* that also clustered with TgPR3 (Fig. 1) is involved in response to mechanical stress [58] as well as to heat, salt and drought stress [59]. AT1G05850 is related to cellulose biosynthesis [60] and also to response to high temperatures, salt and drought stress [59]. Sequences Tc00_t060970, Tc03_t026990, Tc03_t027000, Tc03_t027010 and Tc03_t027030, which were clustered with TgPR5 (Fig. 1), showed increased expression levels during cacao interaction with the pathogenic fungi *P. palmivora* and *Colletotrichum theobromicola* [57]. The *A. thaliana* AT4G11650 sequence showed an increased expression with *Agrobacterium tumefaciens* at 24 hai [61]. This gene is also regulated by the ethylene and jasmonic acid–signalization pathway [62]. Transgenic Arabidopsis plants knocked-out for the transcription factor WRKY33 – which is mediated by ethylene and the jasmonic acid signalization pathway – showed a susceptibility pattern to *Botritys cinerea* and a reduction of AT4G11650 expression level, while the wild-type plants showed increased AT4G11650 expression in response to the pathogen [62]. The *A. thaliana* sequence AT5G24090, homologous to TgPR8 (Fig. 1),

showed an expression pattern specific to stress response; however, no expression was observed during the plant development stage [63]. In *T. cacao*, the Tc03_g017760 gene homologous with TgPR8 (Fig. 1) showed an increased expression level when the plant was inoculated by *P. palmivora* or *Colletotrichum theobromicola* [57]. The PR gene's expression in response to biotic and abiotic stress could be related to the phytohormone pathways that regulate their expression. This could be related to the literature data about *M. perniciosa*, which modifies the metabolism of *T. cacao* during compatible interactions through the phytohormone pathway [64].

4.3 *TgPR* genes were highly expressed in the cupuassu genotype resistant to *M. perniciosa*

The relative expression of *TgPR3*, *TgPR5* and *TgPR8* was highly significant in the resistant genotype infected by *M. perniciosa*, at all of the harvesting points, but mainly at 8 and 24 hai for *TgPR5* (Fig. 3A). In the *T. cacao–M. perniciosa* interaction, which is closely related to and also deeper studied than the cupuassu-*M. perniciosa* pathosystem, the basidiospore germination and the beginning of the germination tube in the plant tissues were observed at 6 hai [65], a time period that is coherent with the high and early expression of the TgPRs (Figs. 3A and B). The very high expression observed for TgPR5 since 8 hai would corroborate other reports, in which the PR5 was overexpressed in resistant plant genotypes after pathogen infection [17, 66-68]. The osmotin's function and mode of action are still unclear, and different functions have been shown, such as in inhibiting beta-glucanase or xylanase [17, 69]. Here, we propose that TgPR5 may act as chitinase due to its strong *in silico* interaction with chitin and chitosan, as well as its extracellular localization (Fig. 2, Table 1). Thus, we the resistant cupuassu genotype may have been able to recognize *M. perniciosa* throught its innate immune system – probably through effectors [70] – and to generate a defense response

against the pathogen from the beginning of the infection process (Fig. 5), which explains why the C174 resistant genotype does not present symptoms or disease features in the field [71]. In the susceptible cupuassu genotype, the TgPR genes showed reduced expression at all of the harvesting times (Fig. 3) showing that the pathogen can bypass the innate immune system of cupuassu and cause virulence. In *T. cacao–M. perniciosa* interaction, the fungus can interfere with the host's metabolism and alter its gene expression [64]. The reduction of plant chitinase expression levels during the cupuassu–*M. perniciosa* interaction can be highly beneficial to the pathogen, which can grow and colonize the plant tissues (Fig. 5). Moreover, the reduction of cell wall degradation by chitinases (i.e. cell wall fragments) reduces the recognition by the plant's innate immune system through chitin receptors [72, 73] (Fig. 5). In contrast, increased plant chitinase expression and secretion can cause serious damage to the pathogen, allowing the plant to recognize the pathogen, and triggering defense mechanisms and the plant's resistance [73] (Fig. 5).

5. Conclusion

Here, we have shown the first *in silico* and *in vitro* analysis of pathogenesis-related proteins from *T. grandiflorum*. We show that TgPR3 and TgPR8 are putative chitinases with distinct structures, and that TgPR5 is a putative osmotin, all with affinity for chitin and chitosan molecules. These results suggest a new role for TgPR5/osmotin as chitinase/chitosanase in plant–pathogen interactions. TgPR expression highly increased in the resistant cupuassu genotype infected *by M. perniciosa* (mainly TgPR5 at the first infection times) and was low in the susceptible one. These results could be related to the phylogenetic analysis of the *TgPR* genes showing that *T. grandiflorum* sequences clustered with cacao and Arabidopsis *PR* sequences are involved in response to biotic and abiotic stress, some through phytohormone-

signaling pathways. These observations suggest that TgPRs could be involved in recognizing mechanisms of a plant's innate immune system through chitin receptors.

Availability of supporting data

The data sets supporting the results of this article are included within the article and its additional files.

Abbreviations: 3D: tridimensional; PAMP: molecular patterns associated with pathogens; PR: pathogenesis related; TLP: thaumatin-like protein

Competing interest

No conflicts of interest to declare.

Authors' contribution

RJSS was responsible for the execution of all the experimental steps. RJSS, LHM and FM analyzed and discussed the data. RJSS and FM wrote the manuscript. KPG and RMA were responsible for plant material production and inoculation with *M. perniciosa*. RMA, LHM, FM and KPG were responsible for the conception and design of the experiments. FM was responsible for the financial support of the research. FM and LHM were responsible for the advising of RJSS.

Acknowledgements

The work of RJSS was supported by the Fundação de Amparo à Pesquisa do Estado da Bahia (FAPESB), the Coordenação de Aperfeiçoamento de Pessoal de Nível Superior (CAPES) and Embrapa Recursos Genéticos e Biotecnologia (Cenargen). This work was supported by

FAPESB project DTE0038/2013. KPG and FM received a Productivity grant from the Conselho Nacional de Desenvolvimento Científico e Tecnológico (CNPq). The authors thank Dr. Akyla Maria Martins Alves for advices during manuscript writing. This work was made in the frame of the International Consortium in Advanced Biology (CIBA).

References

[1] R.M. Alves, M.D.V.d. Resende, B.d.S. Bandeira, T.M. Pinheiro, D.C.R. Farias, Avaliação e seleção de progênies de cupuaçuzeiro (*Theobroma grandiflorum*), em Belém, Pará, Revista Brasileira de Fruticultura, 32 (2010) 204-212.
[2] R.M. Alves, C.R.S. Silva, M.S.C. Silva, D.C.S. Silva, A.M. Sebbenn, Diversidade genética em coleções amazônicas de germoplasma de cupuaçuzeiro [*Theobroma grandiflorum* (Willd. ex Spreng.) Schum.], Revista Brasileira de Fruticultura, 35 (2013) 818-828.
[3] M.C. Costa, G.A. Maia, M.d.S.M. Souza Filho, R.W.d. Figueiredo, R.T. Nassu, J.C.S. Monteiro, Conservação de polpa de cupuaçu [*Theobroma grandiflorum* (Willd. Ex Spreng.) Schum] por métodos combinados, Revista Brasileira de Fruticultura, 25 (2003) 213-215.
[4] R. Sayid, Chocolate Could Run Out In 2020 Due To Worldwide Shortage of Cocoa, in: The Daily Mirror online, 2013, pp. http://www.mirror.co.uk/news/world-news/chocolate-could-run-out-2020-2913505.
[5] A. Wexler, World's sweet tooth heats up cocoa. Growing demand from emerging markets is pushing up prices for key ingredient in chocolate, in: The Wall Street Journal, 2014, pp. http://online.wsj.com/news/articles/SB10001424052702304703804579381234107085804.
[6] R.M. Alves, M.D.V. Resende, Avaliação genética de individuos e progênies de cupuaçuzeiro no estado do Para e estimativas de parâmetros genéticos, Revista Brasileira de Fruticultura, 30 (2008) 696-701.
[7] J. Sels, J. Mathys, B.M.A. De Coninck, B.P.A. Cammue, M.F.C. De Bolle, Plant pathogenesis-related (PR) proteins: a focus on PR peptides, Plant Physiology and Biochemistry, 46 (2008) 941-950.
[8] L.C. Van Loon, Induced resistance in plants and the role of pathogenesis-related proteins, European Journal of Plant Pathology, 103 (1997) 753-765.
[9] S. Ali, B.A. Ganai, A.N. Kamili, A.A. Bhat, Z.A. Mir, J.A. Bhat, A. Tyagi, S.T. Islam, M. Mushtaq, P. Yadav, S. Rawat, A. Grover, Pathogenesis-related proteins and peptides as promising tools for engineering plants with multiple stress tolerance, Microbiological Research, 212-213 (2018) 29-37.
[10] A. Edreva, Pathogenesis-related proteins: Research progress in the last 15 years, Gen Appl Plant Physiology, 31 (2005) 105-124.
[11] M. Sinha, R.P. Singh, G.S. Kushwaha, N. Iqbal, A. Singh, S. Kaushik, P. Kaur, S. Sharma, T.P. Singh, Current overview of allergens of plant pathogenesis related protein families, ScientificWorldJournal, 2014 (2014) 543195-543195.
[12] Hakim, A. Ullah, A. Hussain, M. Shaban, A.H. Khan, M. Alariqi, S. Gul, Z. Jun, S. Lin, J. Li, S. Jin, M.F.H. Munis, Osmotin: A plant defense tool against biotic and abiotic stresses, Plant Physiology and Biochemistry, 123 (2018) 149-159.
[13] J. Grenier, A. Asselin, Sorne Pathogenesis-Related Proteins Are Chitosanases with Lytic Activity Against Fungal Spores, MOLECULAR PLANT-MICROBE INTERACTIONS, 3 (1990) 401-407.
[14] T. Kawase, S. Yokokawa, A. Saito, T. Fujii, N. Nikaidou, K. Miyashita, T. Watanabe, Comparison of Enzymatic and Antifungal Properties between Family 18 and 19 Chitinases from S. coelicolor A3(2), Bioscience, Biotechnology, and Biochemistry, 70 (2006) 988-998.

[15] K. Min, S.C. Ha, P.M. Hasegawa, R.A. Bressan, D.-J. Yun, K.K. Kim, Crystal structure of osmotin, a plant antifungal protein, Proteins: Structure, Function, and Bioinformatics, 54 (2004) 170-173.
[16] D.N. Patil, M. Datta, A. Dev, S. Dhindwal, N. Singh, P. Dasauni, S. Kundu, A.K. Sharma, S. Tomar, P. Kumar, Structural Investigation of a Novel N-Acetyl Glucosamine Binding Chi-Lectin Which Reveals Evolutionary Relationship with Class III Chitinases, PLoS ONE, 8 (2013) e63779.
[17] J.-J. Liu, R. Sturrock, A.M. Ekramoddoullah, The superfamily of thaumatin-like proteins: its origin, evolution, and expression towards biological function, Plant Cell Reports, 29 (2010) 419-436.
[18] T. Pusztahelyi, Chitin and chitin-related compounds in plant-fungal interactions, Mycology, 9 (2018) 189-201.
[19] A. Sánchez-Vallet, J.R. Mesters, B.P.H.J. Thomma, The battle for chitin recognition in plant-microbe interactions, FEMS Microbiology Reviews, 39 (2015) 171-183.
[20] M. Malerba, R. Cerana, Recent Applications of Chitin- and Chitosan-Based Polymers in Plants, Polymers, 11 (2019).
[21] M.S. Riaz Rajoka, L. Zhao, H.M. Mehwish, Y. Wu, S. Mahmood, Chitosan and its derivatives: synthesis, biotechnological applications, and future challenges, Applied Microbiology and Biotechnology, 103 (2019) 1557-1571.
[22] D.S. Gomes, M.A. Lopes, S.P. Menezes, L.F. Ribeiro, C.V. Dias, B.S. Andrade, R.M. de Jesus, A.B.L. Pires, A. Goes-Neto, F. Micheli, Mycelial development preceding basidioma formation in Moniliophthora perniciosa is associated to chitin, sugar and nutrient metabolism alterations involving autophagy, Fungal Genetics and Biology, 86 (2016) 33-46.
[23] M.A. Lopes, D.S. Gomes, M.G. Koblitz, C.P. Pirovani, J.C. Cascardo, A. Goes-Neto, F. Micheli, Use of response surface methodology to examine chitinase regulation in the basidiomycete *Moniliophthora perniciosa*, Mycol Res, 112 (2008) 399-406.
[24] C.S. Souza, B.M. Oliveira, G.G. Costa, A. Schriefer, A. Selbach-Schnadelbach, A.P. Uetanabaro, C.P. Pirovani, G.A. Pereira, A.G. Taranto, J.C. Cascardo, A. Goes-Neto, Identification and characterization of a class III chitin synthase gene of *Moniliophthora perniciosa*, the fungus that causes witches' broom disease of cacao, J Microbiol, 47 (2009) 431-440.
[25] D. Penman, G. Britton, K. Hardwick, H.A. Collin, S. Isaac, Chitin as a measure of biomass of Crinipellis perniciosa, causal agent of witches' broom disease of Theobroma cacao, Mycological Research, 104 (2000) 671-675.
[26] L. Ferraz Dos Santos, R. Moreira Fregapani, L.L. Falcão, R.C. Togawa, M.M.d.C. Costa, U.V. Lopes, K. Peres Gramacho, R.M. Alves, F. Micheli, L.H. Marcellino, First Microsatellite Markers Developed from Cupuassu ESTs: Application in Diversity Analysis and Cross-Species Transferability to Cacao, PLoS ONE, 11 (2016) e0151074-e0151074.
[27] L. Ferraz dos Santos, R.J. Santana Silva, D. Oliveira Jordão do Amaral, M.F. Barbosa de Paula, L. Ludke Falcão, T. Legavre, R.M. Alves, L.H. Marcellino, F. Micheli, Selection of Reference Genes for Expression Study in Pulp and Seeds of Theobroma grandiflorum (Willd. ex Spreng.) Schum, PLoS ONE, 11 (2016) e0160646.
[28] L.L. Falcao, J.O.S. Werneck, R.C. Togawa, M.M.d.C. Costa, P. Grynberg, O.B.d. Silva Junior, R.M. Alves, P.S.B. Albuquerque, L.H. Marcellino, Analyses of cupuassu (*Theobroma grandiflorum*) transcriptome during interaction with *Moniliophthora perniciosa*, the causal agent of Witches' Broom disease., in: S.-E. CPATU (Ed.) 7th BRAZILIAN BIOTECHNOLOGY CONGRESS and 2nd BIOTECHNOLOGY IBERO-AMERICAN CONGRESS, Brasília, DF, Brazil, 2018.
[29] T.N. Petersen, S. Brunak, G. von Heijne, H. Nielsen, SignalP 4.0: discriminating signal peptides from transmembrane regions, Nat Meth, 8 (2011) 785-786.
[30] E. Gasteiger, C. Hoogland, A. Gattiker, S. Duvaud, M.R. Wilkins, R.D. Appel, B. A., Protein Identification and Analysis Tools on the ExPASy Server, in: J.M.W. (ed) (Ed.) The Proteomics Protocols Handbook, Humana Press 2005, pp. 571-607.
[31] S. Briesemeister, J. Rahnenführer, O. Kohlbacher, YLoc--an interpretable web server for predicting subcellular localization, Nucleic Acids Research, 38 (2010) W497-W502.
[32] X. Argout, J. Salse, J.-M. Aury, M.J. Guiltinan, G. Droc, J. Gouzy, M. Allegre, C. Chaparro, T. Legavre, S.N. Maximova, M. Abrouk, F. Murat, O. Fouet, J. Poulain, M. Ruiz, Y. Roguet, M. Rodier-

520 Goud, J.F. Barbosa-Neto, F. Sabot, D. Kudrna, J.S.S. Ammiraju, S.C. Schuster, J.E. Carlson, E. Sallet, T.
521 Schiex, A. Dievart, M. Kramer, L. Gelley, Z. Shi, A. Bérard, C. Viot, M. Boccara, A.M. Risterucci, V.
522 Guignon, X. Sabau, M.J. Axtell, Z. Ma, Y. Zhang, S. Brown, M. Bourge, W. Golser, X. Song, D. Clement,
523 R. Rivallan, M. Tahi, J.M. Akaza, B. Pitollat, K. Gramacho, A. D'Hont, D. Brunel, D. Infante, I. Kebe, P.
524 Costet, R. Wing, W.R. McCombie, E. Guiderdoni, F. Quetier, O. Panaud, P. Wincker, S. Bocs, C.
525 Lanaud, The genome of Theobroma cacao, Nature Genetics, 43 (2011) 101-108.
526 [33] S. Kumar, G. Stecher, M. Li, C. Knyaz, K. Tamura, MEGA X: Molecular Evolutionary Genetics
527 Analysis across Computing Platforms, Molecular Biology and Evolution, 35 (2018) 1547-1549.
528 [34] K. Arnold, L. Bordoli, J. Kopp, T. Schwede, The SWISS-MODEL workspace: a web-based
529 environment for protein structure homology modelling, Bioinformatics, 22 (2006) 195-201.
530 [35] F. MELO, d. Melo, e. melo, g. melo, *ANOLEA*: a www server to assess protein structures, *Intell.*
531 *Sys. Mol. Biol*., 97 (1997) 110-113.
532 [36] R.A. Laskowski, M.W. MacArthur, D.S. Moss, J.M. Thornton, PROCHECK: a program to check the
533 stereochemical quality of protein structures, Journal of Applied Crystallography, 26 (1993) 283-291.
534 [37] M.A. Larkin, G. Blackshields, N.P. Brown, R. Chenna, P.A. McGettigan, H. McWilliam, F. Valentin,
535 I.M. Wallace, A. Wilm, R. Lopez, J.D. Thompson, T.J. Gibson, D.G. Higgins, Clustal W and Clustal X
536 version 2.0, Bioinformatics, 23 (2007) 2947-2948.
537 [38] G.M. Morris, R. Huey, W. Lindstrom, M.F. Sanner, R.K. Belew, D.S. Goodsell, A.J. Olson,
538 AutoDock4 and AutoDockTools4: Automated docking with selective receptor flexibility, Journal of
539 Computational Chemistry, 30 (2009) 2785-2791.
540 [39] O. Trott, A.J. Olson, AutoDock Vina: improving the speed and accuracy of docking with a new
541 scoring function, efficient optimization and multithreading, Journal of Computational Chemistry, 31
542 (2010) 455-461.
543 [40] W.L. DeLano, The PyMOL Molecular Graphics System, in, 2002.
544 [41] E.D. Cruz, R.M. Alvez, R.L. Benchimol, Avaliação de clones de cupuacuzeiro (Theobroma
545 grandiflorum (Willd. ex Spreng) K. Schumm.) quanto a tolerância a vassoura-de-bruxa (Crinipellis
546 perniciosa (Stahel) Singer). in: Embrapa Amazônia Oriental. Comunicado técnico, 28, Embrapa
547 CPATU, Belém, PA, Brazil, 2000, pp. 4 p.
548 [42] S. Surujdeo-Maharaj, P. Umaharan, D.R. Butler, T.N. Sreenivasan, An optimized screening
549 method for identifying levels of resistance to *Crinipellis perniciosa* in cocoa (*Theobroma cacao*), Plant
550 Pathol, 52 (2003) 464-475.
551 [43] G. Frias, L. Purdy, R. Schmidt, An inoculation method for evaluating resistance of cacao to
552 *Crinipellis perniciosa*, Plant Disease, 79 (1995) 787-791.
553 [44] A. Untergasser, H. Nijveen, X. Rao, T. Bisseling, R. Geurts, J.A.M. Leunissen, Primer3Plus, an
554 enhanced web interface to Primer3, Nucleic Acids Research, 35 (2007) W71-W74.
555 [45] B. Thornton, C. Basu, Real-time PCR (qPCR) primer design using free online software,
556 Biochemistry and Molecular Biology Education, 39 (2011) 145-154.
557 [46] S. Zhao, R.D. Fernald, Comprehensive algorithm for quantitative real-time polymerase chain
558 reaction, J Comput Biol, 12 (2005) 1047-1064.
559 [47] C.L. Andersen, J.L. Jensen, T.F. Ørntoft, Normalization of Real-Time Quantitative Reverse
560 Transcription-PCR data: a model-based variance estimation approach to identify genes suited for
561 normalization, applied to bladder and colon cancer data sets, Cancer Research, 64 (2004) 5245-5250.
562 [48] M.W. Pfaffl, G.W. Horgan, L. Dempfle, Relative expression software tool (REST) for group-wise
563 comparison and statistical analysis of relative expression results in real-time PCR, Nucleic Acids
564 Research, 30 (2002) e36-e36.
565 [49] N. Takahashi-Ando, M. Inaba, S. Ohsato, T. Igawa, R. Usami, M. Kimura, Identification of multiple
566 highly similar XIP-type xylanase inhibitor genes in hexaploid wheat, Biochemical and Biophysical
567 Research Communications, 360 (2007) 880-884.
568 [50] S. Martínez-Caballero, P. Cano-Sánchez, I. Mares-Mejía, A.G. Díaz-Sánchez, M.L. Macías-
569 Rubalcava, J.A. Hermoso, A. Rodríguez-Romero, Comparative study of two GH19 chitinase-like
570 proteins from Hevea brasiliensis, one exhibiting a novel carbohydrate-binding domain, The FEBS
571 Journal, 281 (2014) 4535-4554.

[51] T. Ohnuma, N. Umemoto, T. Nagata, S. Shinya, T. Numata, T. Taira, T. Fukamizo, Crystal structure of a “loopless” GH19 chitinase in complex with chitin tetrasaccharide spanning the catalytic center, Biochimica et Biophysica Acta (BBA) - Proteins and Proteomics, 1844 (2014) 793-802.
[52] F. Fukamizo, Chitinolytic Enzymes: Catalysis, Substrate Binding, and their Application, Current Protein & Peptide Science, 1 (2000) 105-124.
[53] T. Masuda, G. Zhao, B. Mikami, Crystal structure of class III chitinase from pomegranate provides the insight into its metal storage capacity, Bioscience, Biotechnology, and Biochemistry, 79 (2015) 45-50.
[54] H. Koiwa, H. Kato, T. Nakatsu, J.i. Oda, Y. Yamada, F. Sato, Crystal structure of tobacco PR-5d protein at 1.8 Å resolution reveals a conserved acidic cleft structure in antifungal thaumatin-like proteins11Edited by R. Huber, Journal of Molecular Biology, 286 (1999) 1137-1145.
[55] M.M. Chaudet, T.A. Naumann, N.P.J. Price, D.R. Rose, Crystallographic structure of ChitA, a glycoside hydrolase family 19, plant class IV chitinase from Zea mays, Protein Science, 23 (2014) 586-593.
[56] N.A. Udaya Prakash, M. Jayanthi, R. Sabarinathan, P. Kangueane, L. Mathew, K. Sekar, Evolution, Homology Conservation, and Identification of Unique Sequence Signatures in GH19 Family Chitinases, Journal of Molecular Evolution, 70 (2010) 466-478.
[57] A.S. Fister, L.C. Mejia, Y. Zhang, E.A. Herre, S.N. Maximova, M.J. Guiltinan, Theobroma cacao L. pathogenesis-related gene tandem array members show diverse expression dynamics in response to pathogen colonization, BMC Genomics, 17 (2016) 363-363.
[58] K. Koizumi, R. Yokoyama, K. Nishitani, Mechanical load induces upregulation of transcripts for a set of genes implicated in secondary wall formation in the supporting tissue of Arabidopsis thaliana, Journal of Plant Research, 122 (2009) 651.
[59] Y. Kwon, S.-H. Kim, M.-S. Jung, M.-S. Kim, J.-E. Oh, H.-W. Ju, K.-i. Kim, E. Vierling, H. Lee, S.-W. Hong, Arabidopsis hot2 encodes an endochitinase-like protein that is essential for tolerance to heat, salt and drought stresses, The Plant Journal, 49 (2007) 184-193.
[60] C. Sánchez-Rodríguez, S. Bauer, K. Hématy, F. Saxe, A.B. Ibáñez, V. Vodermaier, C. Konlechner, A. Sampathkumar, M. Rüggeberg, E. Aichinger, L. Neumetzler, I. Burgert, C. Somerville, M.-T. Hauser, S. Persson, Chitinase-like1/pom-pom1 and its homolog CTL2 are glucan-interacting proteins important for cellulose biosynthesis in Arabidopsis, The Plant Cell, 24 (2012) 589-607.
[61] R.F. Ditt, K.F. Kerr, P. de Figueiredo, J. Delrow, L. Comai, E.W. Nester, The Arabidopsis thaliana Transcriptome in Response to Agrobacterium tumefaciens, Molecular Plant-Microbe Interactions®, 19 (2006) 665-681.
[62] Z. Zheng, S. Qamar, Z. Chen, T. Mengiste, Arabidopsis WRKY33 transcription factor is required for resistance to necrotrophic fungal pathogens, Plant Journal, 48 (2006).
[63] Y. Takenaka, S. Nakano, M. Tamoi, S. Sakuda, T. Fukamizo, Chitinase Gene Expression in Response to Environmental Stresses in Arabidopsis thaliana: Chitinase Inhibitor Allosamidin Enhances Stress Tolerance, Bioscience, Biotechnology, and Biochemistry, 73 (2009) 1066-1071.
[64] P.J.P.L. Teixeira, D.P.d.T. Thomazella, O. Reis, P.F.V. do Prado, M.C.S. do Rio, G.L. Fiorin, J. José, G.G.L. Costa, V.A. Negri, J.M.C. Mondego, P. Mieczkowski, G.A.G. Pereira, High-resolution transcript profiling of the atypical biotrophic interaction between *Theobroma cacao* and the fungal pathogen *Moniliophthora perniciosa*, The Plant Cell, 26 (2014) 4245-4269.
[65] K. Sena, L. Alemanno, K.P. Gramacho, The infection process of *Moniliophthora perniciosa* in cacao, Plant Pathology, (2014) 1272–1281.
[66] D. Prasath, I. El-Sharkawy, S. Sherif, K.S. Tiwary, S. Jayasankar, Cloning and characterization of PR5 gene from Curcuma amada and Zingiber officinale in response to Ralstonia solanacearum infection, Plant Cell Reports, 30 (2011) 1799.
[67] D. PRASATH, A. BALAGOPAL, V. MAHANTESH, O.B. ROSANA, S. JAYANSANKAR, M. ANANDARAJ, Comparative study of pathogenesis-related protein 5 (PR5) of different Zingiberaceae species., Indian Journal of Biotechnology, 13 (2014) 178-185.

[68] A. El-kereamy, I. El-sharkawy, R. Ramamoorthy, A. Taheri, D. Errampalli, P. Kumar, S. Jayasankar, Prunus domestica pathogenesis-related protein-5 activates the defense response pathway and enhances the resistance to fungal infection, PLoS ONE, 6 (2011) e17973-e17973.
[69] J. Grenier, C. Potvin, J. Trudel, A. Asselin, Some thaumatin-like proteins hydrolyse polymeric β-1,3-glucans, The Plant Journal, 19 (1999) 473-480.
[70] C.S. Barbosa, R.R.d. Fonseca, T.M. Batista, M.A. Barreto, C.S. Argolo, M.R.d. Carvalho, D.O.J.d. Amaral, E.M.d.A. Silva, E. Arévalo-Gardini, K.S. Hidalgo, G.R. Franco, C.P. Pirovani, F. Micheli, K.P. Gramacho, Genome sequence and effectorome of Moniliophthora perniciosa and Moniliophthora roreri subpopulations, BMC Genomics, 19 (2018) 509-509.
[71] R.M. Alves, M.D.V. Resende, B.S. Bandeira, T.M. Pinheiro, D.C.R. Farias, Evolução da vassoura-de-bruxa e avaliação da resistência em progênies de cupuaçuzeiro, Revista Brasileira de Fruticultura, 31 (2009) 1022-1032.
[72] H. Böhm, I. Albert, L. Fan, A. Reinhard, T. Nürnberger, Immune receptor complexes at the plant cell surface, Current Opinion in Plant Biology, 20 (2014) 47-54.
[73] H. Kaku, Y. Nishizawa, N. Ishii-Minami, C. Akimoto-Tomiyama, N. Dohmae, K. Takio, E. Minami, N. Shibuya, Plant cells recognize chitin fragments for defense signaling through a plasma membrane receptor, Proceedings of the National Academy of Sciences of the United States of America, 103 (2006) 11086-11091.

Tables

Table 1. TgPR gene and protein sequence characteristics.

Name	Gene data			Protein data						
	Identification*	mRNA * (bp)	ORF size (bp)	Protein size (aa)	Signal peptide (aa)	Molecular weight (kDa)	pI	Subcellular localization (probability)	Phosphorylation sites	Glycosylation sites
TgPR3	C106	1239	966	322	26	35.5	6.64	Extracellular (86.48%)	S_{37} S_{41} S_{114} S_{123} S_{193} T_{91} T_{99} T_{185} T_{205} T_{219} T_{240} Y_{62} Y_{119} Y_{124} Y_{126} Y_{145} Y_{167}	N_{20} N_{171} N_{207}
TgPR5	C68	950	672	224	23	24.2	6.68	Extracellular (99.7%)	S_{118} S_{139} S_{161} S_{176} T_{143} T_{256} Y_{137} Y_{239}	N_{163}
TgPR8	C356	1111	927	309	29	33.3	4.27	Extracellular (52.2%) Vacuolar (34.5%)	S_{77} S_{95} S_{147} S_{266} T_{15} T_{41} T_{88} Y_{66} Y_{99} Y_{134} Y_{149} Y_{162} Y_{227}	N_{145}

* Data from RNA-seq as described by [28].

Figure legends

Figure 1. Phylogenetic tree obtained with the *TgPR* nucleotide sequences and their homologues from *T. cacao* and *A. thaliana*. **A.** Phylogenic tree from *TgPR3*. **B.** Phylogenic tree from *TgPR5*. **C.** Phylogenic tree from *TgPR8*. Sequence names beginning with Tc and AT correspond to *T. cacao* and *A. thaliana*, respectively. The yellow square highlights the TgPR's closest phylogenetic branches.

Figure 2. The 3D structure of TgPR proteins. **A.** TgPR3's 3D structure, with the amino acid residues Lys70 Glu92, and Tyr125 of the active site highlighted. **B.** TgPR5's 3D structure with the amino acid residues Arg43, Glu83, Asp96 and Asp101 of the active site highlighted. **C.** TgPR8's 3D structure with the amino acid residues Tyr6, Phe32, Asp125, Glu127, Gln155, Gln178, Tyr180 and Trp253 of the active site highlighted.

Figure 3. Representations (2D and 3D) of docking between TgPRs and chitin/chitosan.

Figure 4. Relative expression of TgPR genes in resistant (R) and susceptible (S) cupuassu genotypes 8, 24, 48 and 72 hours after inoculation (hai) with *Moniliophthora perniciosa*. **A.** Full-scale representation. **B.** Reduced scale for the best visualization of lower relative expression.

Figure 5. Putative scheme of the early steps (6–72 hai) of the interactions between *T. grandiflorum* plants and the hemibiotrophic fungus *M. perniciosa*. **A.** Resistant interaction. **B.** Susceptible interaction. PTI: PAMP-triggered immunity; ETI: effector-triggered immunity; PRR: pattern-recognition receptors; PR: pathogenesis-related protein; PCD: programmed cell death.

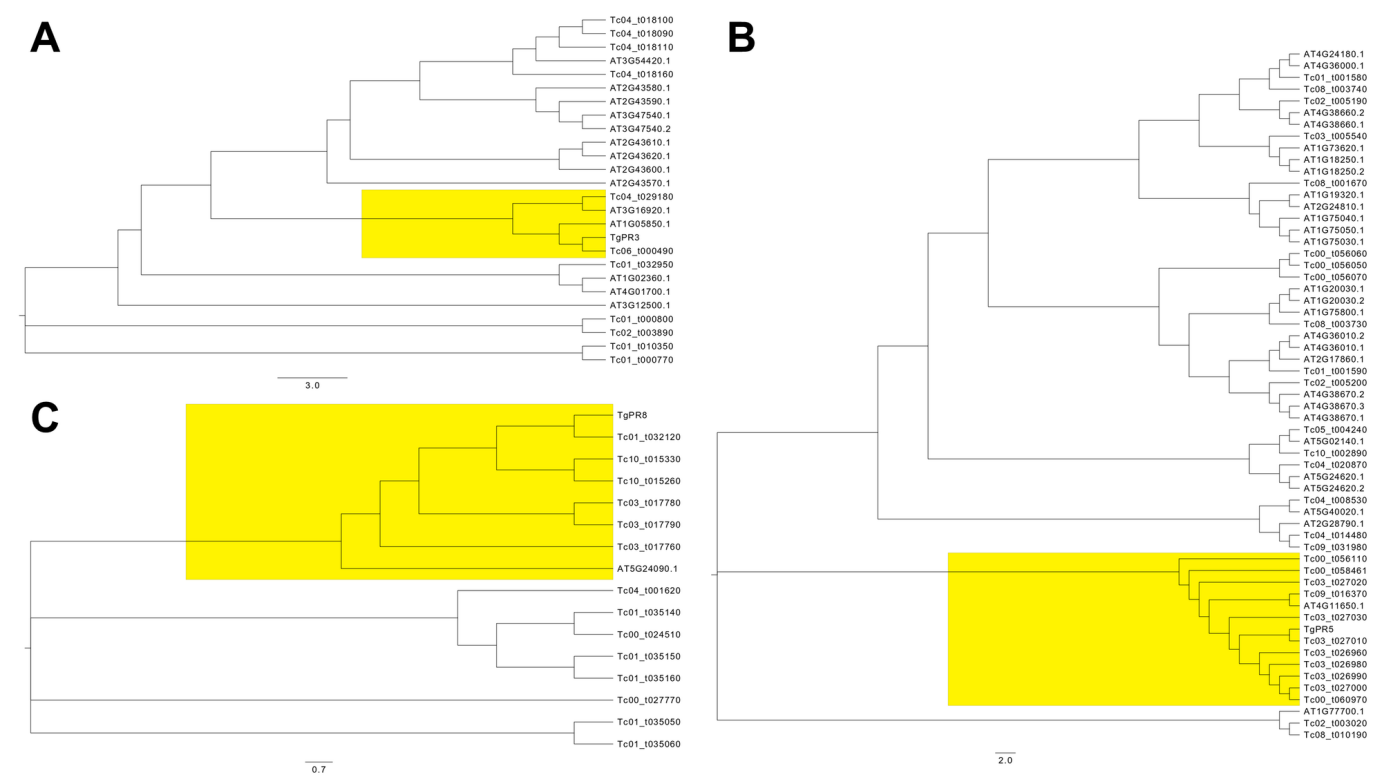
A
Tc04_t018100
Tc04_t018090
Tc04_t018110
AT3G54420.1
Tc04_t018160
AT2G43580.1
AT2G43590.1
AT3G47540.1
AT3G47540.2
AT2G43610.1
AT2G43620.1
AT2G43600.1
AT2G43570.1
Tc04_t029180
AT3G16920.1
AT1G05850.1
TgPR3
Tc06_t000490
Tc01_t032950
AT1G02360.1
AT4G01700.1
AT3G12500.1
Tc01_t000800
Tc02_t003890
Tc01_t010350
Tc01_t000770
3.0
B
AT4G24180.1
AT4G36000.1
Tc01_t001580
Tc08_t003740
Tc02_t005190
AT4G38660.2
AT4G38660.1
Tc03_t005540
AT1G73620.1
AT1G18250.1
AT1G18250.2
Tc08_t001670
AT1G19320.1
AT2G24810.1
AT1G75040.1
AT1G75050.1
AT1G75030.1
Tc00_t056060
Tc00_t056050
Tc00_t056070
AT1G20030.1
AT1G20030.2
AT1G75800.1
Tc08_t003730
AT4G36010.2
AT4G36010.1
AT2G17860.1
Tc01_t001590
Tc02_t005200
AT4G38670.2
AT4G38670.3
AT4G38670.1
Tc05_t004240
AT5G02140.1
Tc10_t002890
Tc04_t020870
AT5G24620.1
AT5G24620.2
Tc04_t008530
AT5G40020.1
AT2G28790.1
Tc04_t014480
Tc09_t031980
Tc00_t056110
Tc00_t058461
Tc03_t027020
Tc09_t016370
AT4G11650.1
Tc03_t027030
TgPR5
Tc03_t027010
Tc03_t026960
Tc03_t026980
Tc03_t026990
Tc03_t027000
Tc00_t060970
AT1G77700.1
Tc02_t003020
Tc08_t010190
2.0
C
TgPR8
Tc01_t032120
Tc10_t015330
Tc10_t015260
Tc03_t017780
Tc03_t017790
Tc03_t017760
AT5G24090.1
Tc04_t001620
Tc01_t035140
Tc00_t024510
Tc01_t035150
Tc01_t035160
Tc00_t027770
Tc01_t035050
Tc01_t035060
0.7

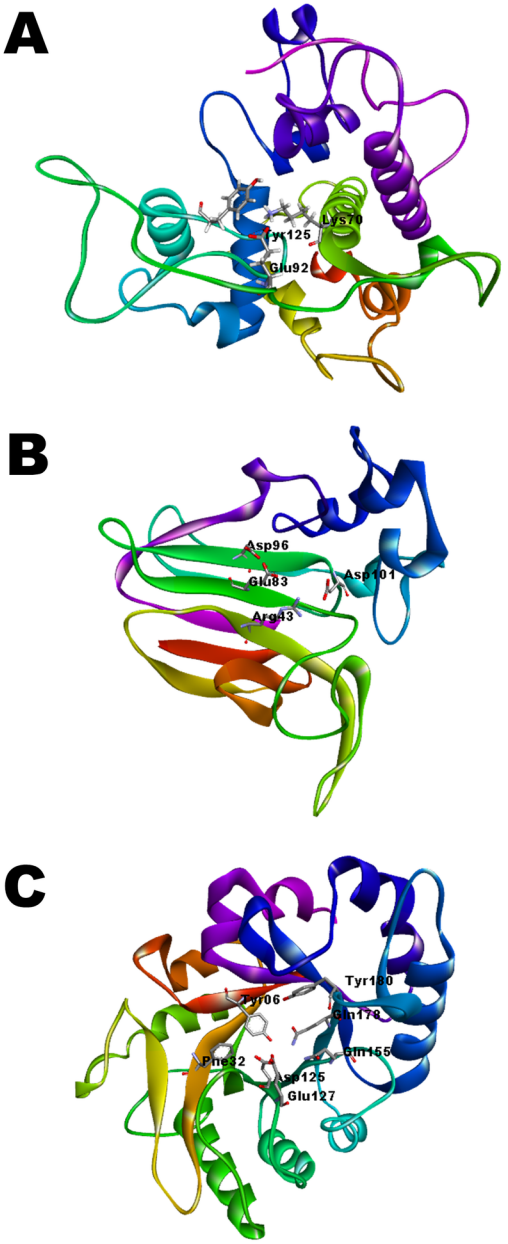
A
Lys70
Tyr125
Glu92
TgPR3
B
Asp96
Glu83
Asp101
Arg43
TgPR5
C
Tyr130
Tyr106
Glu178
Glu155
Phe32
Asp125
Glu127
TgPR8

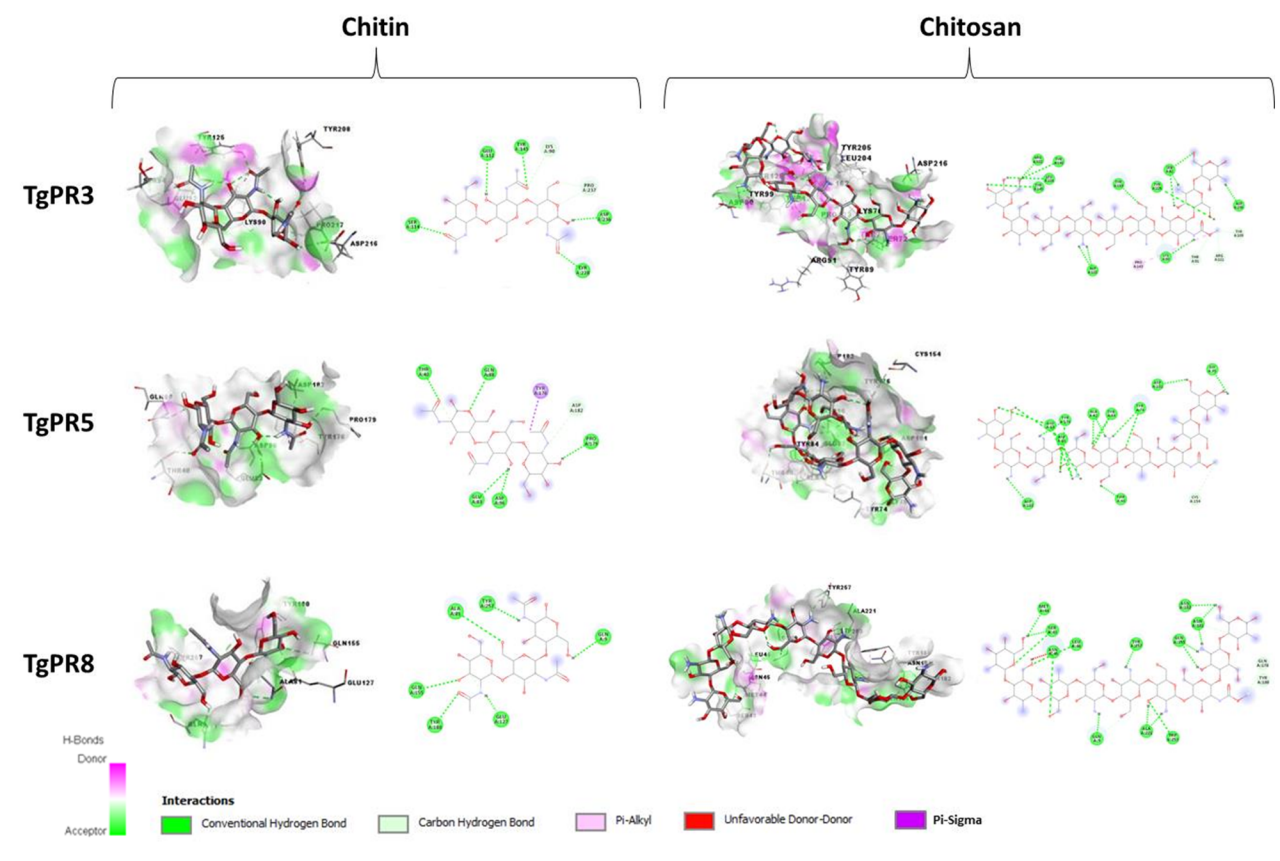
Chitin
Chitosan
TgPR3
TgPR5
TgPR8
TYR208
TYR126
LYS30
PRO212
ASP216
TYR205
LEU204
ASP216
TYR32
LYS74
ARG81
TYR89
CYS164
TYR84
TYR74
TYR150
GLN155
GLU127
TYR267
ALA221
H-Bonds
Donor
Acceptor
Interactions
Conventional Hydrogen Bond
Carbon Hydrogen Bond
Pi-Alkyl
Unfavorable Donor-Donor
Pi-Sigma

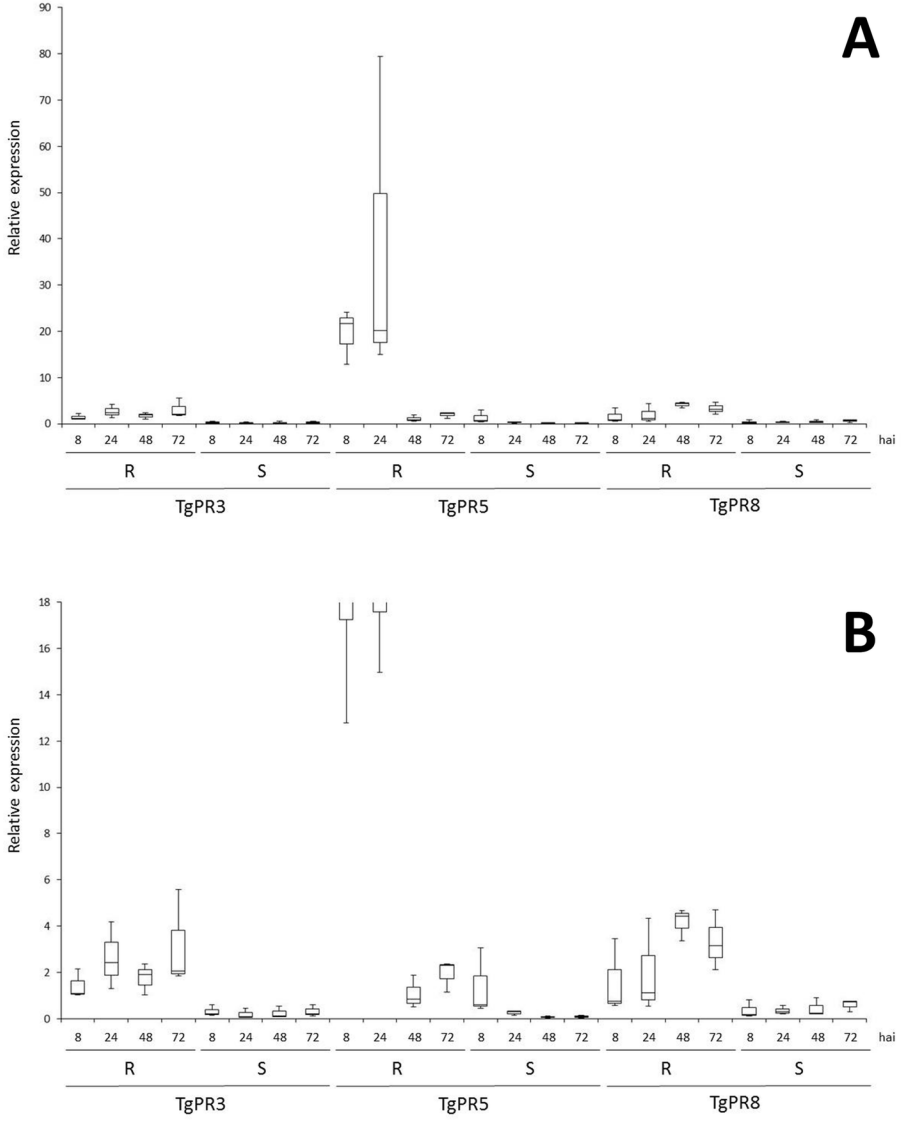
A
Relative expression
90
80
70
60
50
40
30
20
10
0
8 24 48 72 8 24 48 72 8 24 48 72 8 24 48 72 8 24 48 72 8 24 48 72 hai
R S R S R S
TgPR3 TgPR5 TgPR8
B
Relative expression
18
16
14
12
10
8
6
4
2
0
8 24 48 72 8 24 48 72 8 24 48 72 8 24 48 72 8 24 48 72 8 24 48 72 hai
R S R S R S
TgPR3 TgPR5 TgPR8

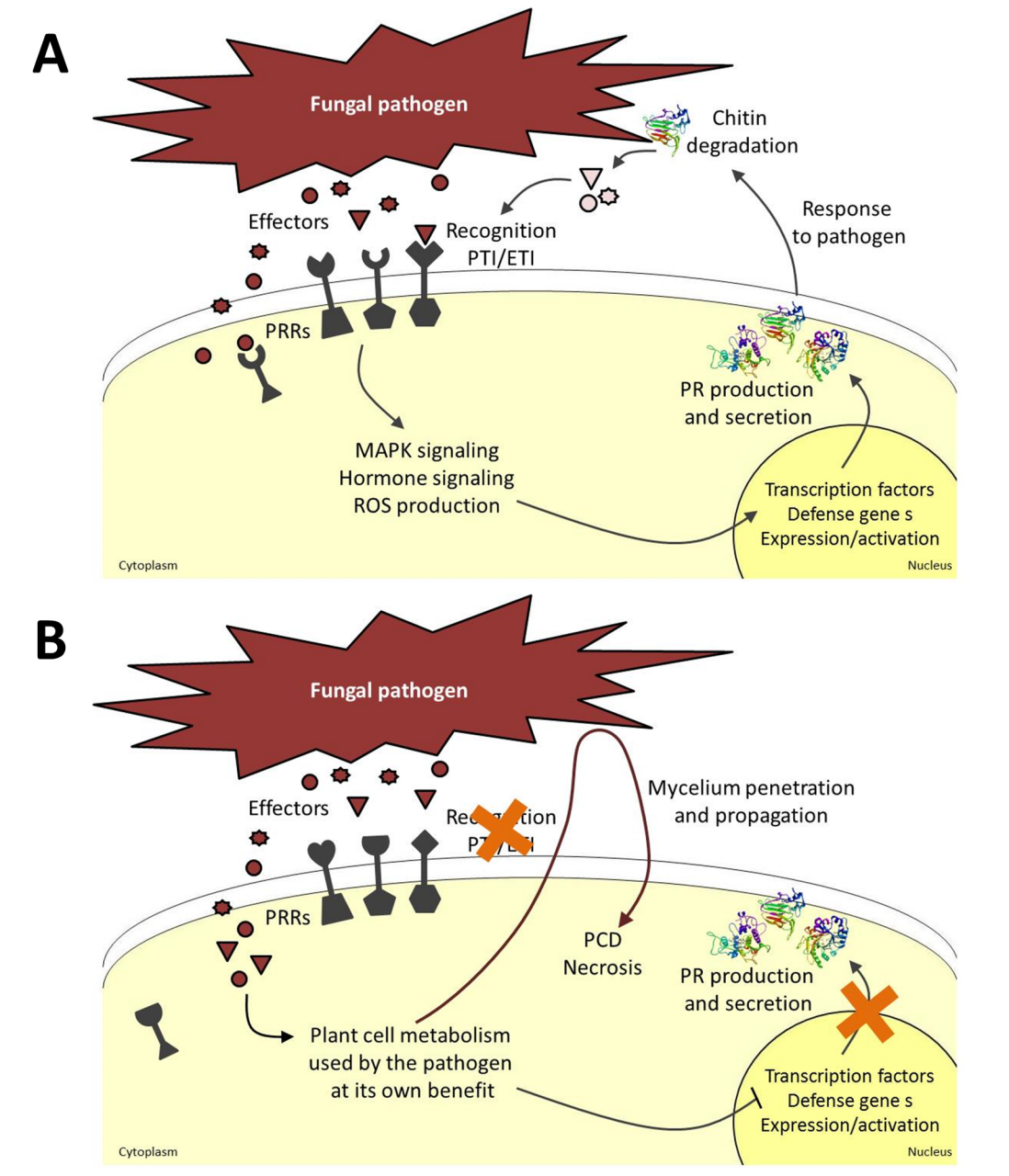
A
Fungal pathogen
Chitin degradation
Effectors
Recognition PTI/ETI
Response to pathogen
PRRs
PR production and secretion
MAPK signaling
Hormone signaling
ROS production
Transcription factors
Defense gene s
Expression/activation
Cytoplasm
Nucleus
B
Fungal pathogen
Effectors
Mycelium penetration and propagation
PRRs
PCD
Necrosis
PR production and secretion
Plant cell metabolism used by the pathogen at its own benefit
Transcription factors
Defense gene s
Expression/activation
Cytoplasm
Nucleus